

EDGESpot: EFFICIENT AND HIGH-PERFORMANCE FEW-SHOT MODEL FOR KEYWORD SPOTTING

Oguzhan Buyuksolak, Alican Gok, Osman Erman Okman

Analog Devices, Istanbul, Turkey

ABSTRACT

We introduce an efficient few-shot keyword spotting model for edge devices, EdgeSpot, that pairs an optimized version of a BC-ResNet-based acoustic backbone with a trainable Per-Channel Energy Normalization frontend and lightweight temporal self-attention. Knowledge distillation is utilized during training by employing a self-supervised teacher model, optimized with Sub-center ArcFace loss. This study demonstrates that the EdgeSpot model consistently provides better accuracy at a fixed false-alarm rate (FAR) than strong BC-ResNet baselines. The largest variant, EdgeSpot-4, improves the 10-shot accuracy at 1% FAR from 73.7% to 82.0%, which requires only 29.4M MACs with 128k parameters.

Index Terms— Few-shot keyword spotting, edge computing, knowledge distillation, self-supervised speech

1. INTRODUCTION

Keyword Spotting (KWS) enables hands-free interaction by detecting specific spoken commands or wake-words in audio, but conventional neural network (NN) based systems require extensive data and significant computational resources during training. Adapting the model for different sets of keywords requires repeating the same training procedure; therefore, it is not feasible to adapt the models on edge hardware. Few-shot keyword spotting (FS-KWS) overcomes these limitations by using deep neural networks with compact architectures and metric learning techniques [1], such as prototypical networks, to recognize new keywords from just a few examples. These systems learn an embedding space where similar keywords cluster together, allowing users to enroll custom keywords with minimal data. In open-set scenarios, users enroll new keywords by providing a small number of spoken samples, which are generally averaged in the embedding space to form

class prototypes [2]. During inference, the system classifies test samples by measuring their proximity to these prototypes.

In [3, 4], a ResNet [5] based model is trained with triplet loss to achieve good FS-KWS application performance. Recently, another training scheme was suggested that leverages Self-supervised learning (SSL) models for robust feature extraction [6]. A teacher–student framework for knowledge distillation is proposed to train the same ResNet architecture from the reduced dimensionality embeddings of the pretrained SSL model. Still, this model architecture is not optimized enough for edge deployment.

However, in the fixed vocabulary KWS literature, there are plenty of options for efficient model architectures [7, 8, 9]. Among them, BC-ResNet [10] has emerged as a state-of-the-art model on the Google Speech Commands (GSC) [11] benchmark, while also offering computational efficiency and scalability. Motivated by the strong efficiency–accuracy trade-offs of this model architecture, we introduce EdgeSpot for the few-shot setting: a compact, edge-friendly model. EdgeSpot augments the BC-ResNet backbone with a trainable Per-Channel Energy Normalization (PCEN) [12] frontend and lightweight temporal self-attention to yield more discriminative embeddings at low false-alarm rates (FAR).

In this work, we provide a comprehensive overview of the proposed architecture, detailing its structure as well as its performance in terms of accuracy and computational efficiency. To ensure a fair comparison, we adapt BC-ResNet to the same FS-KWS training method and prototype-based inference protocol. Furthermore, we analyze the enhancements that EdgeSpot introduces over the baseline ResNet architecture described in [6]. Through side-by-side evaluations, we demonstrate that EdgeSpot consistently outperforms BC-ResNet and the baseline on both the Multilingual Spoken Words Corpus (MSWC) [13] and cross-domain GSC datasets, all while maintaining the low computational and parameter requirements essential for on-device deployment.

2. PROPOSED METHOD

2.1. Model Architecture

EdgeSpot adopts BC-ResNet as its acoustic backbone and introduces three targeted, edge-friendly improvements that raise

© 2026 IEEE. Personal use of this material is permitted. Permission from IEEE must be obtained for all other uses, in any current or future media, including reprinting/republishing this material for advertising or promotional purposes, creating new collective works, for resale or redistribution to servers or lists, or reuse of any copyrighted component of this work in other works.

To appear in Proceedings of the IEEE International Conference on Acoustics, Speech, and Signal Processing (ICASSP), 2026.

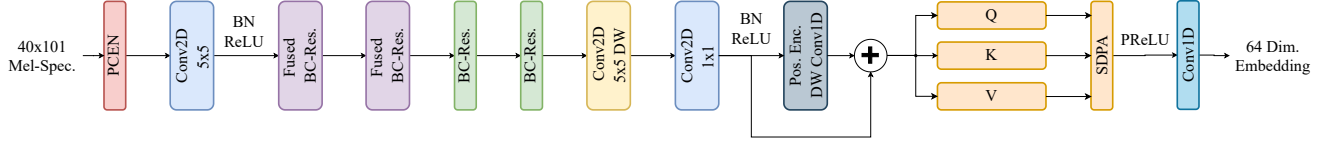


Fig. 1. Architecture of the Proposed Model. The model processes a 40×101 Mel-Spectrogram input and applies Per-Channel Energy Normalization (PCEN) for preprocessing. It then passes through a 5×5 Conv2D layer followed by depthwise 2D convolutions (DW Conv2D) and residual blocks (BC-Res. and Fused BC-Res.) to extract hierarchical features. Positional encoding is incorporated using a depthwise Conv1D layer to enhance temporal feature representation. A self-attention mechanism (SDPA) focuses on capturing dependencies in the time dimension. Finally, a Conv1D layer reduces dimensionality, producing a 64-dimensional embedding as the output.

accuracy while preserving efficiency: (a) an additional trainable PCEN frontend before the acoustic stack, (b) an early-block temporal-path fusion that replaces the depthwise separable convolution with a single temporal convolution, and (c) insertion of a lightweight temporal self-attention head. Fig. 1 and Table 1 present the details of the EdgeSpot architecture. Details are explained in the following sections.

Table 1. Details of the model architecture for $\tau = 1$, where τ is a multiplier that determines the output channel width. The final conv1d layer always has an output channel of 1, regardless of the value of τ .

Input	Operator	n	c	s	d
$1 \times 40 \times 101$	PCEN	—	—	—	—
$1 \times 40 \times 101$	conv2d(5×5)-BN-ReLU	—	16	(2,1)	1
$16 \times 20 \times 101$	Fused BC-ResBlock	2	8	1	1
$8 \times 20 \times 101$	Fused BC-ResBlock	2	12	(2,1)	(1,2)
$12 \times 10 \times 101$	BC-ResBlock	4	16	(2,1)	(1,4)
$16 \times 5 \times 101$	BC-ResBlock	4	20	1	(1,8)
$20 \times 5 \times 101$	DW conv2d(5×5)	—	20	1	1
$20 \times 1 \times 101$	conv2d(1×1)-BN-ReLU	—	32	1	1
32×101	DW conv1d(16) Pos. E.	—	32	1	1
101×32	SDPA-PReLU	—	—	—	—
101×64	conv1d(1)	—	1	—	—

2.1.1. Per-Channel Energy Normalization (PCEN)

PCEN replaces static log compression with per-channel automatic gain control and stabilized root compression. In practice, it applies a causal IIR smoother to the mel energies and then normalizes and compresses them, as specified in Eqs. (1)–(2) below.

$$\text{PCEN}(t, f) = \left(\frac{E(t, f)}{(\epsilon + M(t, f))^\alpha} + \delta \right)^r - \delta^r, \quad (1)$$

$$M(t, f) = (1 - s) M(t - 1, f) + s E(t, f). \quad (2)$$

Here, $E(t, f)$ is the mel-filterbank energy; $M(t, f)$ is a causal per-channel IIR smoother with $s \in (0, 1)$; $\epsilon > 0$ is a small constant; $\alpha \in [0, 1]$ controls AGC strength; and $\delta > 0$,

$r \in (0, 1]$ define the stabilized root compression [12, 14]. All operations are differentiable, enabling end-to-end learning [12].

PCEN reduces loudness dependence, suppresses stationary backgrounds, and enhances onsets; it is widely reported to improve robustness in noisy and far-field speech. Moreover, it tends to Gaussianize magnitude distributions and decorrelate frequency bands, which benefits discriminative models and cross-domain transfer [12, 14]. We include PCEN in EdgeSpot primarily to strengthen cross-domain generalization. In initial ablations, adding only PCEN with no other architectural change improved cross-domain test set performance (GSC, see section 2.2), which we attribute to PCEN’s ability to Gaussianize and whiten spectrogram magnitudes [14].

In EdgeSpot, we place a PCEN layer before the acoustic backbone and train it jointly with the model, learning channel-shared scalars (α, r, δ) and a channel-shared smoothing coefficient s , while fixing $\epsilon = 10^{-6}$.

2.1.2. Fusion of Early Blocks

Fig. 2 (a) presents the BC-ResBlock as given in [10]. The first layer is a 3×1 frequency-depthwise convolution with Sub-Spectral Normalization, which averages the activation along the frequency dimension. It is followed by a temporal depthwise convolution and then by a 1×1 pointwise convolution to broadcast the temporal feature back to 2D. Lastly, an auxiliary 2D residual connection is added to form the output of the block.

In our architecture, for the audio backbone, we adopt the same early-fusion principle with EfficientNetV2 [15], which shows replacing depthwise-separable stacks with a single regular convolution is beneficial in the earliest stages. Therefore, we first define a Fused BC-ResBlock, which replaces the last two layers of BC-ResBlock with a single regular temporal convolution as seen in Fig. 2(b). Note that the new convolution operation is configured with the same kernel, stride, and dilation and with output channels matched to the original 1×1 projection, while leaving the frequency branch, frequency averaging and broadcasting, the auxiliary 2D residual, and the

transition-block behavior unchanged.

We apply this fused temporal path only in the earliest stages (see Fig. 1) to capture the accuracy benefits observed for early-stage fusion in EfficientNetV2 while avoiding the regressions seen when fully fusing all stages [15]. In our setting, the incremental parameters and operations are minimal, since early stages have small channel counts and the fused operation is 1D on the temporal branch, yet the simplification of the separable stack improves optimization in practice.

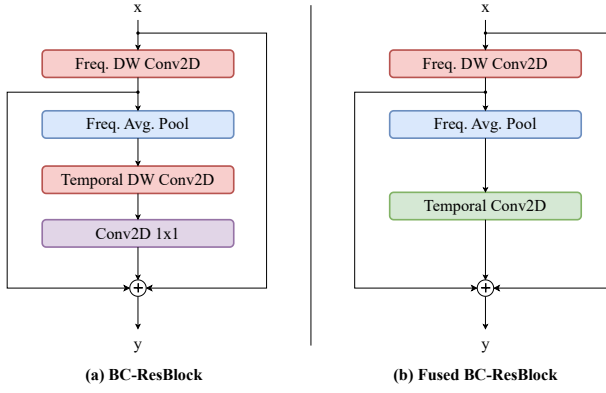


Fig. 2. Comparison of (a) BC-ResBlock and (b) Fused BC-ResBlock, highlighting the replacement of ‘Temporal DW Conv. + 1x1 Conv.’ with a single ‘Temporal Conv.’.

2.1.3. Relative Positional Encoding

To encode temporal order without absolute indices, we use a lightweight, convolutional relative positional encoding along time. Given the channels-first sequence $X \in \mathbb{R}^{C_\tau \times T}$, we add a per-channel depthwise temporal convolution $\varphi(X)$ residually:

$$\tilde{X} = X + \varphi(X), \quad \tilde{X} \in \mathbb{R}^{C_\tau \times T}. \quad (3)$$

This maintains shift equivariance while allowing each channel to learn compact, local timing cues (e.g., onsets/offsets), gently conditioning features for the downstream attention without explicit $T \times T$ positional biases.

The operator $\varphi(\cdot)$ is a depthwise 1D convolution with kernel size κ and “same” padding that preserves the output length:

$$[\varphi(X)]_{c,t} = \sum_{\Delta=-\lfloor \kappa/2 \rfloor}^{\lfloor \kappa/2 \rfloor} K_{c,\Delta} X_{c,t+\Delta}, \quad c = 1, \dots, C_\tau, \quad (4)$$

where $K \in \mathbb{R}^{C_\tau \times \kappa}$ are learnable per-channel filters and out-of-range indices are zero padded. In EdgeSpot, we set $\kappa = 16$ and symmetric padding $p = 8$. The positional-enhanced sequence \tilde{X} is then fed to the attention block (Sec. 2.1.4).

2.1.4. Scaled Dot Product Attention (SDPA)

In EdgeSpot, we apply single-head scaled dot-product self-attention along the time axis to model long-range temporal dependencies at low cost for the short utterances considered in KWS. Let the output of the convolutional front-end be a 1D temporal sequence with T frames and C_τ channels, where C_τ depends on the width multiplier τ of the network (see Fig. 1 and Table 1). We reshape this tensor to $X \in \mathbb{R}^{T \times C_\tau}$, i.e., one C_τ -dimensional feature vector per time step.

We first obtain queries, keys, and values via learnable linear projections to a fixed $d = 64$ -dimensional space:

$$Q = XW_Q + \mathbf{1}b_Q^\top, \quad K = XW_K + \mathbf{1}b_K^\top, \quad V = XW_V + \mathbf{1}b_V^\top, \quad (5)$$

where $W_Q, W_K, W_V \in \mathbb{R}^{C_\tau \times d}$, $b_Q, b_K, b_V \in \mathbb{R}^d$, and $\mathbf{1} \in \mathbb{R}^T$ is an all-ones column vector that broadcasts the biases across time. In EdgeSpot, these projections map the backbone activations to $d = 64$ by design, independently of τ .

Scaled dot-product attention over the temporal dimension is then computed as

$$A = \text{Softmax}\left(\frac{QK^\top}{\sqrt{d}}\right) \in \mathbb{R}^{T \times T}, \quad Z = AV \in \mathbb{R}^{T \times d}, \quad (6)$$

where the \sqrt{d} scaling stabilizes gradients for large d and the softmax is applied row-wise so that each row of A forms a probability distribution over time steps. In our implementation, the attention strictly operates along the temporal axis (no spatial/frequency mixing), consistent with the 1D temporal representation before attention.

We then apply a pointwise nonlinearity to the contextualized sequence,

$$\tilde{Z} = \text{PReLU}(Z), \quad (7)$$

and produce an utterance-level 64-D embedding by aggregating \tilde{Z} across time with a lightweight 1D convolutional head (see Fig. 1):

$$\mathbf{e} = g_\theta(\tilde{Z}) \in \mathbb{R}^{64}, \quad (8)$$

where g_θ denotes the learned temporal aggregation module with a shallow Conv1D stack in EdgeSpot. This head preserves the 64-dimensional embedding size used by our training pipeline and downstream prototype-based inference.

2.2. Training Methodology

We follow the FS-KWS teacher–student pipeline from our prior work [6], in which a pretrained Wav2Vec2.0 encoder [16] provides frame-level features and an attention-based dimensionality reduction head maps them to 64-D embeddings trained with Sub-center ArcFace (SCAF) [17], forming the teacher. The EdgeSpot student is trained end-to-end by distillation from teacher embeddings with a composite objective as:

$$\mathcal{L} = \mathcal{L}_{\text{KD}} + \lambda \mathcal{L}_{\text{SCAF}}, \quad (9)$$

Table 2. Model performance on MSWC (1-/10- shot) and GSC (1-/10- shot). Each cell reports $\text{mean}_{1\text{-shot}}/\text{mean}_{10\text{-shot}}$ with std as a tiny superscript.

Model	MSWC			GSC			#MACs	#Params
	$DET_{1\%}$	$DET_{5\%}$	AUROC	$ACC_{1\%}$	$ACC_{5\%}$	AUC		
Shots	1-/10- shot			1-/10- shot				
Teacher [6]	$91.4^{\pm 0.03}/97.0^{\pm 0.09}$	$97.4^{\pm 0.02}/99.3^{\pm 0.05}$	$99.3^{\pm 0.01}/99.8^{\pm 0.01}$	$65.1^{\pm 7.6}/83.0^{\pm 0.5}$	$75.1^{\pm 6.9}/85.2^{\pm 0.5}$	$82.7^{\pm 5.7}/90.9^{\pm 0.7}$	63.3* G	217.8* M
ResNet15 [6]	$86.3^{\pm 0.13}/96.1^{\pm 0.05}$	$93.9^{\pm 0.03}/98.4^{\pm 0.02}$	$98.3^{\pm 0.01}/99.5^{\pm 0.01}$	$44.3^{\pm 7.4}/75.4^{\pm 1.4}$	$60.6^{\pm 8.0}/85.2^{\pm 0.8}$	$73.7^{\pm 6.9}/91.0^{\pm 0.5}$	235 M	480 k
BC-ResNet-1	$61.2^{\pm 0.08}/81.2^{\pm 0.05}$	$85.3^{\pm 0.08}/95.5^{\pm 0.13}$	$97.0^{\pm 0.01}/98.9^{\pm 0.01}$	$14.1^{\pm 3.9}/35.6^{\pm 2.7}$	$27.3^{\pm 5.6}/52.9^{\pm 2.5}$	$48.5^{\pm 6.6}/71.7^{\pm 1.7}$	2.5 M	10.9 k
Edgespot-1	$66.8^{\pm 0.13}/85.7^{\pm 0.10}$	$88.9^{\pm 0.17}/96.7^{\pm 0.01}$	$97.7^{\pm 0.01}/99.2^{\pm 0.01}$	$17.2^{\pm 4.6}/40.1^{\pm 2.5}$	$28.0^{\pm 6.0}/54.5^{\pm 2.2}$	$50.8^{\pm 7.0}/74.6^{\pm 1.4}$	4.5 M	16.6 k
BC-ResNet-2	$77.3^{\pm 0.17}/91.1^{\pm 0.09}$	$93.3^{\pm 0.14}/98.2^{\pm 0.03}$	$98.5^{\pm 0.01}/99.5^{\pm 0.01}$	$25.8^{\pm 5.4}/53.4^{\pm 2.5}$	$42.0^{\pm 6.8}/69.0^{\pm 1.6}$	$62.9^{\pm 6.7}/83.1^{\pm 0.9}$	7.3 M	30.6 k
Edgespot-2	$79.3^{\pm 0.22}/92.0^{\pm 0.12}$	$94.0^{\pm 0.08}/98.4^{\pm 0.02}$	$98.6^{\pm 0.01}/99.5^{\pm 0.01}$	$29.2^{\pm 5.6}/57.1^{\pm 2.2}$	$48.2^{\pm 6.6}/74.0^{\pm 1.2}$	$66.8^{\pm 6.2}/85.7^{\pm 1.0}$	10.3 M	43.3 k
BC-ResNet-3	$83.5^{\pm 0.03}/94.0^{\pm 0.18}$	$95.5^{\pm 0.05}/98.8^{\pm 0.04}$	$98.9^{\pm 0.01}/99.6^{\pm 0.01}$	$36.8^{\pm 7.0}/68.4^{\pm 1.4}$	$56.6^{\pm 8.0}/79.7^{\pm 0.8}$	$73.7^{\pm 7.1}/89.2^{\pm 0.5}$	14.5 M	59.2 k
Edgespot-3	$85.2^{\pm 0.19}/94.8^{\pm 0.22}$	$95.9^{\pm 0.22}/98.9^{\pm 0.04}$	$99.0^{\pm 0.01}/99.7^{\pm 0.01}$	$41.1^{\pm 8.0}/70.2^{\pm 1.6}$	$57.2^{\pm 8.3}/80.8^{\pm 0.9}$	$73.2^{\pm 6.3}/89.4^{\pm 0.4}$	18.6 M	80.6 k
BC-ResNet-4	$87.1^{\pm 0.26}/95.5^{\pm 0.08}$	$96.4^{\pm 0.05}/99.1^{\pm 0.03}$	$99.1^{\pm 0.01}/99.7^{\pm 0.01}$	$44.5^{\pm 7.6}/73.7^{\pm 1.2}$	$60.5^{\pm 7.8}/82.1^{\pm 0.6}$	$74.3^{\pm 7.1}/90.6^{\pm 0.4}$	24.1 M	96.6 k
Edgespot-4	$87.8^{\pm 0.12}/95.7^{\pm 0.06}$	$96.7^{\pm 0.04}/99.1^{\pm 0.01}$	$99.2^{\pm 0.01}/99.7^{\pm 0.01}$	$51.8^{\pm 8.1}/82.0^{\pm 0.9}$	$67.0^{\pm 7.8}/87.4^{\pm 0.6}$	$79.0^{\pm 6.6}/91.9^{\pm 0.4}$	29.4 M	128.3 k

* The teacher model consists of a Wav2vec2 encoder up to the 16th transformer layer and the dimensionality reduction module.

where \mathcal{L}_{KD} is the MSE between teacher and student embeddings, with $\lambda = 5 \times 10^{-5}$. To train the networks, we use the train split of the English portion of MSWC, which contains 5.5 million 1-second samples of 39,000 unique words. We test our approach using the MSWC dataset’s test split, comprised of 680k samples from 38,090 unique words, and the cross-domain GSC dataset, a collection of 100k 1-second audio clips belonging to 35 short commands. For student models, each 1-second waveform (16 kHz) is converted to a 40-band mel spectrogram using a centered STFT, yielding a 40×101 frequency-time map that serves as input to the acoustic front end.

A keyword prototype is formed by averaging embeddings from K examples; and the decision is made by comparing the inference results against the keyword prototypes. A threshold is used to control the FAR, following the same protocol as given in [6]. Models are trained for 40 epochs, using the Adam optimizer with weight decay 4×10^{-5} and a cosine learning-rate schedule. The first 5 epochs linearly warm up to a peak learning rate of 1×10^{-3} , after which cosine decay is applied at every optimization step. We apply SpecAugment [18] during training with settings tied to model width. For the smallest model ($\tau = 1$), no SpecAugment is used, including time-stretch. For $\tau \in \{2, 3, 4\}$, we enable SpecAugment with time-stretch factors sampled uniformly from $[0.9, 1.1]$, a frequency-mask width $F = 6$, and a time-mask width $T = 8$.

3. EXPERIMENTAL RESULTS

We evaluate EdgeSpot against BC-ResNet baselines under the same prototype-based FS-KWS protocol as our prior work [6]. For fairness, we adapt BC-ResNet to the FS-KWS setting by replacing the final classifier to produce 64-dimensional embeddings compatible with our KD setup.

Table 2 summarizes 1-shot and 10-shot results on MSWC and GSC. For GSC, we used 100 random trials with K-shot enrollments of the 11 target keywords (including silence) against the remaining 25 words. For MSWC, we utilize 3 independent runs, and each run consists of 100,000 positive and negative examples each.

On MSWC, we evaluate performance using $\text{DET}@X$, defined as the detection rate at a FAR of X . EdgeSpot consistently outperforms the re-trained BC-ResNet baselines under the same FS-KWS protocol, with the largest gains at low FARs and in the 1-shot setting. EdgeSpot-4 closely follows the Teacher, particularly on $\text{DET}@5\%$ and AUROC, with only a small gap at $\text{DET}@1\%$ in both 1-shot and 10-shot settings. Moreover, EdgeSpot-4 surpasses ResNet15 on nearly all metrics.

Cross-domain tests on GSC further highlight the benefits of the proposed architecture. EdgeSpot improves over BC-ResNet at all scales, most notably at $\text{FAR}=1\%$, and EdgeSpot-4 outperforms ResNet15 on all metrics. With 10-shot enrollment, EdgeSpot-4 attains near-Teacher performance and even exceeds it at more relaxed operating points. In the 1-shot case, the Teacher remains best, yet EdgeSpot-4 narrows the gap substantially relative to BC-ResNet, demonstrating strong transfer despite distribution shift.

4. DISCUSSION

We evaluated EdgeSpot under the same prototype-based FS-KWS protocol as our prior work [6] and, for fairness, re-trained BC-ResNet baselines with the identical KD+SCAF loss tailored to FS-KWS. EdgeSpot delivers higher low-FAR accuracy than BC-ResNet on both MSWC and cross-domain GSC with minimal additional on-device cost. Notably, EdgeSpot-4 outperforms the ResNet15 baseline accuracy with fewer computational requirements, and nearly matches

the SSL Teacher across all metrics, especially on GSC in the 10-shot condition. On MSWC, performance at relaxed operating points is effectively saturated relative to the Teacher. In the more challenging 1-shot regime, the Teacher remains strongest as expected, yet EdgeSpot-4 substantially narrows the gap while consistently outperforming BC-ResNet.

Overall, these findings demonstrate that EdgeSpot, when distilled with SCAF, recovers much of the Teacher’s discriminative power at strict FARs, while preserving an edge-friendly resource footprint.

5. REFERENCES

[1] Mark Mazumder, Colby Banbury, Josh Meyer, Pete Warden, and Vijay Janapa Reddi, “Few-shot keyword spotting in any language,” in *Interspeech*, 2021, pp. 4214–4218.

[2] Dongjune Lee, Minchan Kim, Sung Hwan Mun, Min Hyun Han, and Nam Soo Kim, “Fully unsupervised training of few-shot keyword spotting,” in *2022 IEEE Spoken Language Technology Workshop (SLT)*, 2023, pp. 266–272.

[3] Manuele Rusci and Tinne Tuytelaars, “On-device customization of tiny deep learning models for keyword spotting with few examples,” *IEEE Micro*, vol. 43, no. 6, pp. 50–57, 2023.

[4] Manuele Rusci and Tinne Tuytelaars, “Few-shot open-set learning for on-device customization of keyword spotting systems,” in *Proc. Interspeech*, 2023, pp. 2768–2772.

[5] Kaiming He, Xiangyu Zhang, Shaoqing Ren, and Jian Sun, “Deep residual learning for image recognition,” *CoRR*, vol. abs/1512.03385, 2015.

[6] Alican Gok, Oguzhan Buyuksolak, Osman Erman Okman, and Murat Sarclar, “Enhancing few-shot keyword spotting performance through pre-trained self-supervised speech models,” *arXiv preprint arXiv:2506.17686*, 2025.

[7] Somshubra Majumdar and Boris Ginsburg, “MatchboxNet: 1D time-channel separable convolutional neural network architecture for speech commands recognition,” in *Proc. Interspeech*, 2020, pp. 3356–3360.

[8] Menglong Xu and Xiao-Lei Zhang, “Depthwise separable convolutional resnet with squeeze-and-excitation blocks for small-footprint keyword spotting,” in *Interspeech 2020*, 2020, pp. 2547–2551.

[9] Seungwoo Choi, Seokjun Seo, Beomjun Shin, Hyeong-min Byun, Martin Kersner, Beomsu Kim, Dongyoung Kim, and Sungjoo Ha, “Temporal convolution for real-time keyword spotting on mobile devices,” in *Proc. Interspeech*, 2019, pp. 3372–3376.

[10] Byeonggeun Kim, Simyung Chang, Jinkyu Lee, and Dooyong Sung, “Broadcasted residual learning for efficient keyword spotting,” in *Proc. Interspeech 2021*, 2021, pp. 4538–4542.

[11] Pete Warden, “Speech commands: A dataset for limited-vocabulary speech recognition,” *arXiv preprint arXiv:1804.03209*, 2018.

[12] Yuxuan Wang, Pascal Getreuer, Thad Hughes, Richard F. Lyon, and Rif A. Saurous, “Trainable frontend for robust and far-field keyword spotting,” *CoRR*, vol. abs/1607.05666, 2016.

[13] Mark Mazumder, Sharad Chitlangia, Colby Banbury, Yiping Kang, Juan Manuel Ciro, Keith Achorn, Daniel Galvez, Mark Sabini, Peter Mattson, David Kanter, et al., “Multilingual spoken words corpus,” in *Thirty-fifth Conference on Neural Information Processing Systems Datasets and Benchmarks Track (Round 2)*, 2021.

[14] Vincent Lostanlen, Justin Salamon, Mark Cartwright, Brian McFee, Andrew Farnsworth, Steve Kelling, and Juan Pablo Bello, “Per-channel energy normalization: Why and how,” *IEEE Signal Processing Letters*, vol. 26, no. 1, pp. 39–43, 2019.

[15] Mingxing Tan and Quoc Le, “Efficientnetv2: Smaller models and faster training,” in *International conference on machine learning*. PMLR, 2021, pp. 10096–10106.

[16] Alexei Baevski, Yuhao Zhou, Abdelrahman Mohamed, and Michael Auli, “wav2vec 2.0: A framework for self-supervised learning of speech representations,” in *Advances in Neural Information Processing Systems*, 2020, vol. 33, pp. 12449–12460.

[17] Jiankang Deng, Jia Guo, Tongliang Liu, Mingming Gong, and Stefanos Zafeiriou, “Sub-center arcface: Boosting face recognition by large-scale noisy web faces,” in *European Conference on Computer Vision (ECCV)*, 2020, pp. 741–757.

[18] Daniel S Park, William Chan, Yu Zhang, Chung-Cheng Chiu, Barret Zoph, Ekin D Cubuk, and Quoc V Le, “Specaugment: A simple data augmentation method for automatic speech recognition,” *arXiv preprint arXiv:1904.08779*, 2019.